

UC Davis

UC Davis Previously Published Works

Title

White Matter Hyperintensities and Their Penumbra Lie Along a Continuum of Injury in the Aging Brain

Permalink

<https://escholarship.org/uc/item/0648495c>

Journal

Stroke, 45(6)

ISSN

0039-2499

Authors

Maillard, Pauline
Fletcher, Evan
Lockhart, Samuel N
[et al.](#)

Publication Date

2014-06-01

DOI

10.1161/strokeaha.113.004084

Peer reviewed

Published in final edited form as:

Stroke. 2014 June ; 45(6): 1721–1726. doi:10.1161/STROKEAHA.113.004084.

White Matter Hyperintensities and their Penumbra Lie Along a Continuum of Injury In The Aging Brain

Pauline Maillard, PhD^{1,2}, Evan Fletcher, PhD^{1,2}, Sam N. Lockhart, B.S.^{1,2}, Alexandra E. Roach, M.S.^{1,2}, Bruce Reed, PhD^{1,2}, Dan Mungas, PhD^{1,2}, Charles DeCarli, MD^{1,2}, and Owen Carmichael, PhD^{1,2}

¹Imaging of Dementia and Aging Laboratory, University of California, Davis

²Department of Neurology and Center for Neuroscience, University of California, Davis

Abstract

Background and Purpose—Aging is accompanied by clinically-silent cerebral white matter injury identified through white matter hyperintensities (WMHs) on FLAIR and diffusion tensor imaging (DTI) based measures of WM integrity. The temporal course of FLAIR and DTI changes within WMHs and their less-injured periphery (i.e. their penumbra), however, has not been fully studied. We used longitudinal DTI and FLAIR to explore these changes.

Methods—115 participants, aged 73.7±6.7 years, received clinical evaluations and MRIs on two dates. WMHs and fractional anisotropy (FA) maps were produced from FLAIR and DTI and coregistered to a standardized space. Each distinct WMH was categorized as growing, stagnant or noncontiguous incident. The penumbra of each WMH was similarly categorized as corresponding to a stagnant, growing or noncontiguous incident WMH. Linear mixed-effect models were used to assess whether FA and FLAIR measurements changed between baseline and follow-up and differed between tissue categories.

Results—Baseline FA differed significantly by tissue category, with the following ordering of categories from highest to lowest FA: penumbra of noncontiguous incident, then stagnant, then growing WMHs; noncontiguous incident, then stagnant, then growing WMHs. Despite differences in baseline values, all tissue categories experienced declines in FA over time. Only noncontiguous incident WMHs showed significant FLAIR signal increases over time, and FLAIR signal significantly *decreased* in stagnant WMHs.

Conclusions—WMHs and their penumbra vary in severity, and together span a continuous spectrum of WM injury that worsens with time. FLAIR fails to fully capture this continuous injury process but does identify a sub-class of lesions that appear to improve over time.

Introduction

There is now a substantial body of evidence that clinically silent brain injury, including Magnetic Resonance Imaging (MRI) infarction, white matter hyperintensities (WMH) on

Address correspondence: Owen Carmichael, Center for Neuroscience, 1544 Newton Court, Davis, CA, 95817-2307, USA, Phone: 530-754-9657, Fax: 530-754-5036, ocarmichael@ucdavis.edu.

Conflict of Interest/Disclosure: The authors report no actual or potential conflicts of interest in relation to this manuscript.

fluid attenuated inversion recovery (FLAIR) MRI, subtle white matter (WM) injury apparent on diffusion tensor imaging (DTI), and tissue atrophy on T1-weighted MRI, accrues insidiously beginning in middle age¹, and is associated with increased risk of clinically manifest neurological conditions late in life, including stroke, dementia, and cognitive decline²⁻⁵. Therefore, preventing or slowing such silent brain injury has emerged as major goal of current research.

Modifying the course of WMH accrual has received particular attention due to evidence that lesions may arise from clinically-silent cerebrovascular injury, and therefore may be preventable or modifiable through treatment of vascular risk factors^{6, 7}. We have previously used DTI to show that WMHs represent a core of severe WM injury surrounded by a region of WM that is more mildly injured⁸. We introduced a new term, “WMH penumbra” to describe this specific WMH surrounding region. While this term is not yet universally adopted, and subsequent work uses different terminology for the same phenomenon (cite de Groot), we continue to use the term here. This mildly injured periphery is differentially vulnerable to future conversion to WMH^{9, 10}. Among community-dwelling elders with prevalent WMHs, such extensions of WMHs into adjacent tissue represent as much as 80% of the accrued WMH volume over time, and greater extension is associated with greater concurrent cognitive decline⁴. These findings suggest that WMH penumbra may represent a clinically-relevant target for interventions that arrest the progression of WMHs.

However, any effort to arrest WMH accrual among individuals with prevalent WMHs depends critically on how the white matter injury represented by WMHs and their penumbra evolves over time. While penumbra are at increased risk of conversion to WMH, it is unclear whether penumbra actually differ from WMH in terms of their vulnerability to future injury: white matter integrity within WMHs themselves may continue to decrease over time after they are identified as WMHs, or they may have already reached effective “floor” levels of tissue integrity. It is also unclear how much heterogeneity there is among WMHs and penumbra in terms of such future changes. Better understanding whether WMH and their penumbra truly differ in terms of prognosis, or whether they simply represent different points on a continuum of degeneration severity, could clarify the usefulness of separating WMH and penumbra into separate tissue categories, and targeting one or the other for interventions.

To our knowledge, no studies to date have tracked the temporal course of WM integrity change within both WMHs and their penumbra to better understand their prognoses. To accomplish this, we utilized longitudinal FLAIR and DTI imaging in 115 cognitively normal individuals. In addition, based on our previous observation that appropriately normalized FLAIR signal intensities may provide a continuous measure of white matter integrity similar to FA⁹ we tested whether FA and FLAIR have a complementary or redundant role in describing the WM degeneration process occurring within WMH and their penumbra.

Materials and methods

Sample

The sample included 115 community-dwelling individuals who received comprehensive clinical evaluations according to standardized criteria at the Alzheimer's Disease Center at the University of California, Davis. The present sample included only individuals who were classified as cognitively normal at both baseline and follow-up with no clinically significant cognitive impairment identified based on detailed medical history, neurological examination and neuropsychological testing using the UDS battery. In addition, all subjects received a standardized MRI scan of the brain at two different dates (mean, SD inter-scan interval: 3.3, 1.6 years). The Institutional Review Boards at all participating institutions approved this study, and subjects gave written informed consent. Table 1 summarizes participant characteristics.

Image acquisition and processing

All brain imaging was performed at the University of California, Davis Imaging Research Center on a 1.5-T GE Signa Horizon LX Echospeed system. Three sequences were used: a 3-dimensional T1-weighted coronal spoiled gradient-recalled echo acquisition, a FLAIR sequence, and DTI using the diffusion tensor weighted echo-planar sequence (DTI-EPI; Stanford University, CA). All image acquisition was performed according to previously reported methods^{11, 12}.

Fractional anisotropy (FA) maps were calculated from baseline and follow-up DTI exams and warped to a DTI template. Segmentation of WMH was performed on baseline and follow-up FLAIR images in their native space by a semi-automated procedure previously described^{12, 13}. FLAIR images were then linearly aligned to the corresponding T1-weighted scan using a previously-described image registration method¹¹. The T1-weighted scan was then warped to a T1-weighted template defined in the same space as the DTI template¹⁴, thus allowing FLAIR and T1 images as well as WMH maps to be placed in the same coordinate frame (please see <http://stroke.ahajournals.org> for Supplemental Methods).

Normalizing FLAIR and FA intensities

Normalized FLAIR (nFL) maps were then created by normalizing the intensity distributions of all warped FLAIR images to account for the arbitrary absolute scaling of FLAIR intensities within each scan. Intensities were scaled to set the mean in image intensity within the cranial vault to fixed reference values. All FA values were normalized using a previously described method⁹ that indexes FA at each voxel against healthy young adult FA values at that voxel, to account for inter-voxel FA differences that are due solely to inter-voxel differences in the intrinsic organization of underlying WM tracts¹¹. In such normalized FA (nFA) maps, values less than 1 indicate that the subject exhibits reduced FA there compared to FA values the young reference group exhibited at that location.

A 2-year follow-up nFA map was computed for each subject by interpolating FA values between baseline and follow-up nFA values at a two-year follow-up time point. The same method was used to compute 2-year follow-up nFL maps.

Categorization of WMHs

A first objective of this study was to characterize the time course of nFA and nFL change within WMHs. To understand these changes and how they related to changes in the WMHs themselves, we first placed individual WMHs into categories according to whether or not the lesions grew over time. To do so, distinct WMHs were labeled on the baseline WMH maps in template space and corresponding WMHs were identified on follow-up WMH maps; noncontiguous incident WMHs were labeled on follow-up maps as well⁴. Lesions 5 mm³ or less in volume were excluded from analysis. All other lesions were then placed into three categories: 1) baseline WMH that did not get larger over time were labeled stagnant WMH, 2) baseline WMH that grew larger over time were labeled growing WMH and (3) WMH identified only on follow-up scans were labeled noncontiguous incident WMH (see Figure 1).

Categorization of WMH penumbra

The second objective was to characterize how nFA and nFL change within penumbra. Based on our previous findings⁸, we categorized all white matter voxels within 8 mm of a WMH as its penumbra; voxels within 8 mm of one or more WMHs were assigned to the nearest WMH. To better understand penumbra integrity changes and how they related to changes to the corresponding WMH, each penumbra was assigned to a category based on the category of the WMH including (1) the penumbra of stagnant WMH; (2) the penumbra of growing WMHs and (3) the penumbra of noncontiguous incident WMH (see Figure 1).

Statistical analysis

Descriptive statistics of WMH and penumbra categories—For each individual, overall WMH volumes were computed for the three WMH categories, log-transformed to normalize population variance and compared using pairwise paired t-test.

WMH analysis—The first goal of this analysis was to characterize, at a lesion level, differences between baseline and follow-up nFA and nFL within the three WMH categories. To do so, we calculated mean nFA and mean nFL within each distinct lesion in baseline and follow-up images. We then conducted linear mixed-effects regression with lesion mean nFA or lesion mean nFL as the dependent variable. To determine whether nFA and nFL differed between WMH categories at baseline, we entered WMH category (stagnant, growing and noncontiguous incident WMH) as a fixed effect. To determine whether nFA and nFL changed significantly over time regardless of WMH category, we entered session (baseline vs. follow-up) as a fixed effect. To determine whether 2-year change in nFA and nFL differed between WMH categories, the interaction between WMH category and session was also included.

WMH penumbra analysis—The second goal of analysis was to characterize, at the level of individual penumbra, differences in baseline and follow-up nFA and nFL within the three penumbra categories (Penumbra of Stagnant, Growing, and Noncontiguous incident WMH). To do so, we calculated mean baseline and follow-up nFA and nFL within each distinct penumbra. We then conducted linear mixed-effects regression with mean penumbra nFA or nFL as the dependent variable. Analogous to the WMH analysis, we entered penumbra

category as a fixed effect to identify differences in nFA and nFL between categories. We entered session as a fixed effect to identify changes in nFA and nFL over time across all categories, as well as the interaction of category and session.

Both models included age and hypertension as nuisance covariates, as both have been reported to be associated with FA¹. Multiple measurements per subject generally result in the correlated errors that are explicitly forbidden by the assumptions of standard (between-subjects) AN(C)OVA and regression models. Mixed effects models flexibly give correct estimates of fixed effects in the presence of the correlated errors that arise from a data hierarchy, by controlling for the effects of individual and eventual nested effects. Therefore, the models used in the present study also specified nested random effect of lesion id (or lesion penumbra id) within subject for the intercept as well as for the slope associated with Session effect.

Statistical analyses were performed using R version 2.13.0 (R Development Core Team, 2009, Vienna, Austria).

Results

Descriptive statistics of WMH

Analysis of the total volume of each WMH type within individual brains suggests inter-lesion heterogeneity and confirmation of previous findings related to longitudinal WMH change⁴. The total volume of growing WMH (range: [3.4×10^{-3} ; 38.40]) was significantly larger ($p < 0.001$, on log-transformed volumes) than the volume of noncontiguous incident WMH ([0.027; 1.14]). The volume of stagnant WMH ($[6.7 \times 10^{-3}$; 16.33]) was less than that of growing WMHs ($p < 0.001$) but still substantial, suggesting that WMHs are heterogeneous in terms of change over time.

Baseline and change in DTI and FLAIR among WMH categories

DTI—At baseline, mean nFA within WMHs that went on to subsequently grow over time was lower than that of WMHs that remained stagnant (mean \pm SD: 0.882 ± 0.16 vs. 0.897 ± 0.16 , $p = 0.043$; Figure 2) and that of non-WMH voxels that became noncontiguous incident WMHs during the follow-up period (0.902 ± 0.19 , $p < 0.001$). In contrast, nFA decreased significantly over time among all WMH categories ($\beta = -0.012/\text{year}$, $p < 0.001$) and the amount of decrease did not significantly differ between categories ($p = 0.56$). The mean nFA estimates at baseline and follow-up suggested that the three categories covered a continuum of values that differed at baseline according to category, but not rate of change. For example, mean nFA of noncontiguous incident WMH at follow-up was similar to mean nFA of baseline stagnant WMH; similarly mean nFA of follow-up stagnant WMH values was similar to mean nFA of baseline growing WMH.

FLAIR—At baseline, mean nFL within growing WMHs was greater than that of stagnant WMHs (mean \pm SD: 142.52 ± 16.04 vs. 137.42 ± 13.66 , $p < 0.001$, Figure 2), which in turn was greater than the mean nFL of voxels that subsequently became noncontiguous incident WMHs (118.83 ± 13.74 , $p < 0.001$). However, among WMH categories, only noncontiguous incident WMH showed significant increases in nFL over time ($\beta = 8.16/\text{year}$, $p < 0.001$), while

mean nFL within stagnant WMHs decreased significantly over time ($\beta=-4.08/\text{year}$, $p<0.001$). Growing WMH did not show significant changes in mean nFL over time ($\beta=-0.01/\text{year}$, $p=0.99$). Unlike mean nFA, mean nFL values at baseline and follow-up did not span a continuous range of values across WMH categories.

Baseline and change in DTI and FLAIR among Penumbra categories

DTI—At baseline, nFA was significantly lower in the penumbra of growing WMHs compared to the penumbra of stagnant WMHs (mean \pm SD: 0.908 ± 0.09 vs. 0.916 ± 0.09 , $p=0.046$), which in turn was significantly lower than the nFA of voxels that became the penumbra of noncontiguous incident WMH (0.923 ± 0.012 , $p=0.0203$, see Figure 2). Similar to the WMH categories, nFA within each penumbra category also declined significantly over time ($\beta=-6.1\times 10^{-3}/\text{year}$, $p=0.048$), but rates of change were not significantly different across penumbra categories ($p=0.36$). Similar to the WMH categories, baseline and follow-up mean nFA values suggested that the three penumbra categories spanned a continuum of values. For example mean nFA among voxels that became penumbra of noncontiguous incident WMHs were not significantly different to the baseline mean nFA of stagnant WMH penumbra, and the follow-up mean nFA of stagnant WMH penumbra were not significantly different to the baseline mean nFA of the penumbra of growing WMHs. The follow-up mean nFA of the penumbra of growing WMHs, in turn, was similar to the baseline mean nFA of voxels that went on to become WMHs between baseline and follow-up.

FLAIR—At baseline, nFL was significantly greater in the penumbra of growing WMHs compared to that of the penumbra of stagnant WMHs (mean \pm SD: 108.23 ± 7.5 vs. 106.78 ± 7.9 , $p<0.001$), which in turn was significantly greater than the nFL of voxels that became the penumbra of lesions that emerged between baseline and follow-up (102.85 ± 8.48 , $p<0.001$, see Figure 2). However, only nFL in the penumbra of growing WMHs and voxels that became the penumbra of noncontiguous incident WMH experienced a significant increase in nFL over time ($\beta=0.53/\text{year}$, $p=0.0044$ and $\beta=1.43/\text{year}$, $p<0.001$).

Discussion

This study had four key findings. First, WMHs, their penumbra, and normal white matter all showed similar decline in white matter integrity over time as measured by DTI. Second, WMHs and penumbra were heterogeneous with respect to the severity of white matter injury they represented, with differing categories of novel, stagnant, and growing lesions spanning a continuous spectrum of injury severity as measured by DTI. Third, FLAIR and DTI differed with respect to signal changes over time: unlike DTI, only tissue that became noncontiguous incident WMHs experienced major FLAIR changes over time, and there were major gaps in FLAIR signal values between tissue categories. Fourth, the class of WMHs that did not grow over time had FLAIR signal values that actually improved (decreased) over time. We discuss the significance of each finding in turn.

Similarity of white matter integrity changes in WMHs, penumbra, and normal white matter

In aging, WMHs are usually conceptualized as loci where the white matter has been irrevocably injured. More recently, we and others have introduced the concept of WMH

penumbra as areas surrounding WMHs whose white matter integrity is more subtly reduced, and that are more vulnerable than other healthy WM to convert to WMHs over time. These two concepts led us to hypothesize that WMH penumbra are high-priority targets for intervention as they are potentially amenable to treatment, while WMHs are not. This hypothesis is especially relevant given that the time course of development of WMHs may be modifiable through treatment of vascular risk factors¹⁵⁻¹⁷. However, the findings of this study suggest that this hypothesis is flawed: not only do WMHs have measurable losses of white matter integrity over time, but these losses are similar in magnitude to those of both penumbra and healthy WM. The implication of this finding is that all white matter, including WMHs, may be viewed as vulnerable to integrity loss over time, and potentially viable targets for intervention strategies aimed at slowing or halting such losses.

Heterogeneity of diffusion MRI properties within WMHs and penumbra

The spatial distribution¹⁸ and overall burden⁷ of WMHs, as well as their relationships of WMH burden to vascular risk factors and genetics¹⁹, are known to be heterogeneous. Additionally, the signal properties of certain MRI sequence types—including DTI, FLAIR and magnetization transfer imaging-- within WMHs have also been shown to be heterogeneous, reflecting heterogeneity in the pathological substrate^{20, 21}. For example, differences in MRI signals have been reported between periventricular and deep WMH²², and between confluent and punctuate lesions²³. Magnetic resonance spectroscopy studies have similarly shown such signal heterogeneity²⁴. Our study confirms and extends these findings in two ways. First, we characterized the previously reported heterogeneity of WMHs diffusion MRI as graded differences in white matter integrity between growing, stagnant, and noncontiguous incident lesions. In addition, we showed that for FLAIR, such signal heterogeneity extended longitudinally, while for diffusion MRI it did not: that is, the rate of change in FLAIR signal properties varied by lesion type, while all lesion types showed similar rates of change in the diffusion MRI signal. Because greater MRI signal severity within WMHs may have clinical implications for cognitive impairment²⁵, there is an ongoing need to continue to characterize WMH heterogeneity, both in terms of etiology and in terms of severity of tissue damage. The present study suggests that characterizing the severity of white matter injury by separately quantifying the burden of noncontiguous incident, stagnant, and growing lesions, as well as their corresponding penumbra may help to achieve this goal.

FLAIR and DTI provide differing information

There are now two substantial, almost completely separate bodies of work on the DTI and FLAIR properties of the aging brain²⁶. It has never been clear whether the two techniques provide essentially the same or differing information about the white matter, both because FLAIR studies dichotomize the image signal into hyperintense and normo-intense categories rather than examine the signal as a continuous entity; and because co-collection of DTI and FLAIR is rare. Our findings suggest that DTI captures a continuously evolving, almost linear, process of white matter change in the aging brain. Conversely, we found that FLAIR is more dichotomous; the most healthy and the most severe tissue categories had categorically low and high signal values respectively, as well as minimal changes over time. The implication of this finding is that studies wishing to quantify the full range of white

matter changes, including the earliest declines from peak adult white matter integrity values in middle age or earlier¹ should rely on DTI rather than FLAIR to do so.

Improvement in stagnant lesions

The discovery of stagnant lesions that appear to “improve” slightly over the study interval was a unique finding of our study. Resolving inflammation is one plausible mechanism that could explain the FLAIR signal decreases seen in stagnant lesions: that is, degenerating myelin (myelin “debris”) may trigger the recruitment of glia to clear the debris²⁷; the high concentration of lipid-proton-rich myelin debris would be expected to cause an elevated FLAIR signal which then resolves following debris clearance. However, the true mechanism underlying such improvement is currently unknown and warrants further study.

Limitations

There are limitations to our findings. First, we only measured DTI and FLAIR at two time points, and are therefore unable to assess whether tissue may go through a series of categorical changes, such as changes from normal white matter, to penumbra, and onward to WMH as would be suggested by our model of a continuum of white matter injury. Secondly, we excluded very small (<5mm³) from the analysis. Third, WMH categories (growing, stable or noncontiguous incident) were determined in template space, which may have led, because of interpolation bias produced during registration steps, to miscategorization. To assess this issue, we also performed WMH categorization in FLAIR native space and the results did not significantly differ from those presented in the present paper. Finally, we did not include the anatomical territory of WMH occurrence in the analyses. Any of these additional data items have the potential to more carefully characterize FLAIR changes over time and how these relate to DTI changes.

Summary/Conclusions

The present study provides in vivo evidence that age-related WM lesions and their penumbra can be graded by white matter injury severity, change similarly over time, and lie along a continuum of white matter injury. We also found that FLAIR and DTI have differing measurement properties that may make one or the other technique more appropriate to deploy depending on the scientific question.

Supplementary Material

Refer to Web version on PubMed Central for supplementary material.

Acknowledgments

Source of Funding: The study was supported by NIH grants K01AG030514, R01AG010220, R01AG031563, R01AG021028 and P30AG010129

References

1. Maillard P, Seshadri S, Beiser A, Himali JJ, Au R, Fletcher E, et al. Effects of systolic blood pressure on white-matter integrity in young adults in the framingham heart study: A cross-sectional study. *Lancet Neurol.* 2012; 11:1039–1047. [PubMed: 23122892]

2. Debette S, Beiser A, DeCarli C, Au R, Himali JJ, Kelly-Hayes M, et al. Association of mri markers of vascular brain injury with incident stroke, mild cognitive impairment, dementia, and mortality: The framingham offspring study. *Stroke*. 2010; 41:600–606. [PubMed: 20167919]
3. Wen W, Sachdev PS. Extent and distribution of white matter hyperintensities in stroke patients: The sydney stroke study. *Stroke*. 2004; 35:2813–2819. [PubMed: 15499036]
4. Maillard P, Carmichael O, Fletcher E, Reed B, Mungas D, Decarli C. Coevolution of white matter hyperintensities and cognition in the elderly. *Neurology*. 2012; 79:442–448. [PubMed: 22815562]
5. Lo RY, Jagust WJ. Alzheimer's Disease Neuroimaging I. Vascular burden and alzheimer disease pathologic progression. *Neurology*. 2012; 79:1349–1355. [PubMed: 22972646]
6. Jeerakathil T, Wolf PA, Beiser A, Massaro J, Seshadri S, D'Agostino RB, et al. Stroke risk profile predicts white matter hyperintensity volume: The framingham study. *Stroke*. 2004; 35:1857–1861. [PubMed: 15218158]
7. DeCarli C, Massaro J, Harvey D, Hald J, Tullberg M, Au R, et al. Measures of brain morphology and infarction in the framingham heart study: Establishing what is normal. *Neurobiol Aging*. 2005; 26:491–510. [PubMed: 15653178]
8. Maillard P, Fletcher E, Harvey D, Carmichael O, Reed B, Mungas D, et al. White matter hyperintensity penumbra. *Stroke*. 2011; 42:1917–1922. [PubMed: 21636811]
9. Maillard P, Carmichael O, Harvey D, Fletcher E, Reed B, Mungas D, et al. Flair and diffusion mri signals are independent predictors of white matter hyperintensities. *AJNR Am J Neuroradiol*. 2013; 34:54–61. [PubMed: 22700749]
10. de Groot M, Verhaaren BF, de Boer R, Klein S, Hofman A, van der Lugt A, et al. Changes in normal-appearing white matter precede development of white matter lesions. *Stroke*. 2013; 44:1037–1042. [PubMed: 23429507]
11. Lee DY, Fletcher E, Martinez O, Ortega M, Zozulya N, Kim J, et al. Regional pattern of white matter microstructural changes in normal aging, mci, and ad. *Neurology*. 2009; 73:1722–1728. [PubMed: 19846830]
12. Carmichael O, Mungas D, Beckett L, Harvey D, Tomaszewski Farias S, Reed B, et al. Mri predictors of cognitive change in a diverse and carefully characterized elderly population. *Neurobiol Aging*. 2012; 33:83–95. [PubMed: 20359776]
13. DeCarli C, Fletcher E, Ramey V, Harvey D, Jagust WJ. Anatomical mapping of white matter hyperintensities (wmh): Exploring the relationships between periventricular wmh, deep wmh, and total wmh burden. *Stroke*. 2005; 36:50–55. [PubMed: 15576652]
14. Kochunov P, Lancaster JL, Thompson P, Woods R, Mazziotta J, Hardies J, et al. Regional spatial normalization: Toward an optimal target. *J Comput Assist Tomogr*. 2001; 25:805–816. [PubMed: 11584245]
15. Godin O, Tzourio C, Maillard P, Mazoyer B, Dufouil C. Antihypertensive treatment and change in blood pressure are associated with the progression of white matter lesion volumes: The three-city (3c)-dijon magnetic resonance imaging study. *Circulation*. 2011; 123:266–273. [PubMed: 21220733]
16. Dufouil C, Chalmers J, Coskun O, Besancon V, Bousser MG, Guillon P, et al. Effects of blood pressure lowering on cerebral white matter hyperintensities in patients with stroke: The progress (perindopril protection against recurrent stroke study) magnetic resonance imaging substudy. *Circulation*. 2005; 112:1644–1650. [PubMed: 16145004]
17. Hajjar I, Brown L, Mack WJ, Chui H. Impact of angiotensin receptor blockers on alzheimer disease neuropathology in a large brain autopsy series. *Arch Neurol*. 2012; 69:1632–1638. [PubMed: 22964777]
18. Yoshita M, Fletcher E, Harvey D, Ortega M, Martinez O, Mungas DM, et al. Extent and distribution of white matter hyperintensities in normal aging, mci, and ad. *Neurology*. 2006; 67:2192–2198. [PubMed: 17190943]
19. Raz N, Yang Y, Dahle CL, Land S. Volume of white matter hyperintensities in healthy adults: Contribution of age, vascular risk factors, and inflammation-related genetic variants. *Biochim Biophys Acta*. 2012; 1822:361–369. [PubMed: 21889590]
20. Salat DH. The declining infrastructure of the aging brain. *Brain connectivity*. 2011; 1:279–293. [PubMed: 22432418]

21. O'Sullivan M, Rich PM, Barrick TR, Clark CA, Markus HS. Frequency of subclinical lacunar infarcts in ischemic leukoaraiosis and cerebral autosomal dominant arteriopathy with subcortical infarcts and leukoencephalopathy. *AJNR Am J Neuroradiol.* 2003; 24:1348–1354. [PubMed: 12917126]
22. Spilt A, Goekoop R, Westendorp RG, Blauw GJ, de Craen AJ, van Buchem MA. Not all age-related white matter hyperintensities are the same: A magnetization transfer imaging study. *AJNR Am J Neuroradiol.* 2006; 27:1964–1968. [PubMed: 17032876]
23. Fazekas F, Kleinert R, Offenbacher H, Schmidt R, Kleinert G, Payer F, et al. Pathologic correlates of incidental mri white matter signal hyperintensities. *Neurology.* 1993; 43:1683–1689. [PubMed: 8414012]
24. Constans JM, Meyerhoff DJ, Norman D, Fein G, Weiner MW. 1h and 31p magnetic resonance spectroscopic imaging of white matter signal hyperintensity areas in elderly subjects. *Neuroradiology.* 1995; 37:615–623. [PubMed: 8748891]
25. Chabriat H, Pappata S, Poupon C, Clark CA, Vahedi K, Poupon F, et al. Clinical severity in cadasil related to ultrastructural damage in white matter: In vivo study with diffusion tensor mri. *Stroke.* 1999; 30:2637–2643. [PubMed: 10582990]
26. Gunning-Dixon FM, Brickman AM, Cheng JC, Alexopoulos GS. Aging of cerebral white matter: A review of mri findings. *Int J Geriatr Psychiatry.* 2009; 24:109–117. [PubMed: 18637641]
27. Clarner T, Diederichs F, Berger K, Denecke B, Gan L, van der Valk P, et al. Myelin debris regulates inflammatory responses in an experimental demyelination animal model and multiple sclerosis lesions. *Glia.* 2012; 60:1468–1480. [PubMed: 22689449]

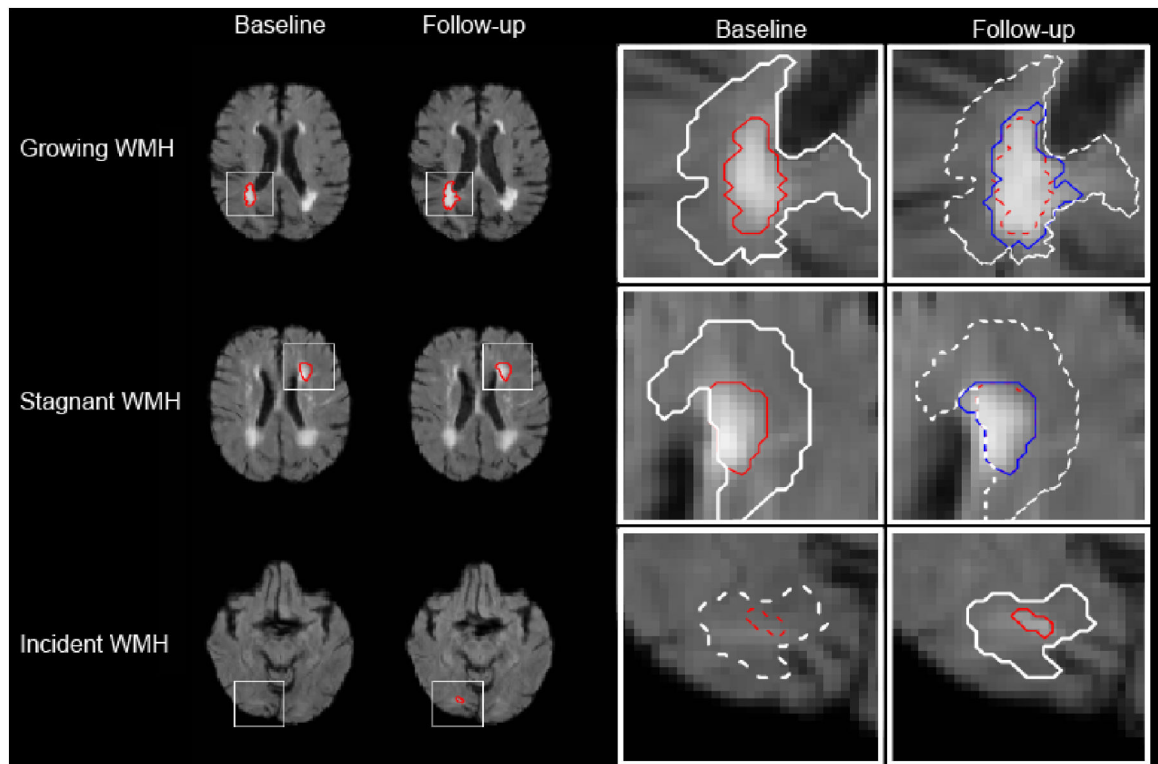


Figure 1.

Example of WMH tissue categorization. Individual lesions (delineated by red boundaries) and the associated lesion penumbra (white boundary) are depicted in baseline and follow-up FLAIR images, as well as the respective expanded views (first to fourth columns respectively). The boundaries of growing and stagnant WMHs as they appear in follow-up images are shown in blue. The boundaries of baseline stagnant and growing WMHs and penumbra are overlaid onto follow-up images in dashed-line contours. The boundaries of noncontiguous incident WMH and penumbra are overlaid onto the baseline image in dashed-line contours.

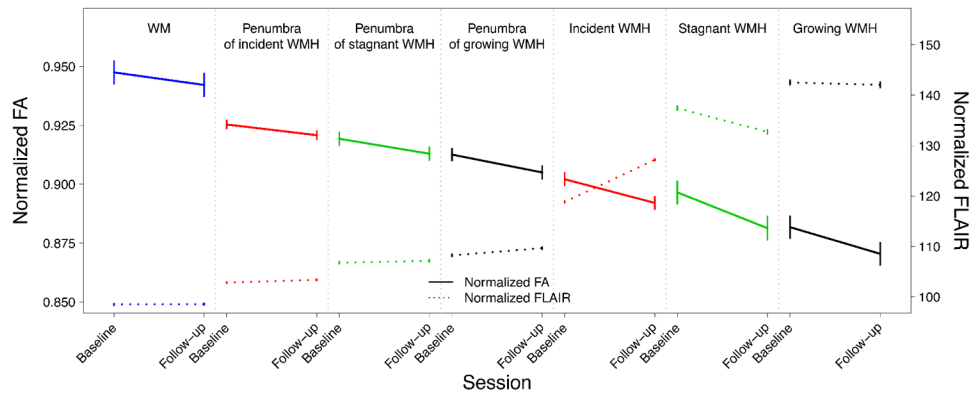


Figure 2. Mean baseline and 2-years follow-up normalized FA (plain line, left side scale) and FLAIR (dot line, right side scale) of the WMH- and WMH penumbra-tracking categories: growing WMH and growing-WMH penumbra (black), stagnant WMH and stagnant-WMH penumbra (green) and noncontiguous incident WMH and noncontiguous incident-WMH penumbra (red). The same measures were computed in normal WM (blue) for visual comparison only.

Table 1

Summary of subject characteristics. Data is presented as mean \pm SD.

Variables	All
Number of subjects	115
Age, y	73.7 \pm 6.7
Years of Education	12.8 \pm 4.7
Gender (# male; % male)	26; 30
History of Hypertension (#; %)	76; 66.6
History of Diabetes (#; %)	36; 31.6
Inter-scan time interval (y)	3.3 \pm 1.6
Baseline brain matter volume (cc)	896.5 \pm 99.9
Baseline WMH volume (cc)	5.7 \pm 8.9